

Down Syndrome: Multimodality Imaging of Associated Congenital Anomalies and Acquired Diseases

Ai Peng Tan, MD, FRCR, MMed(Diag Rad)

Registrar, National University Hospital, Diagnostic Radiology, 5 Lower Kent Ridge Road, Singapore 119074, Singapore

SUMMARY

Down syndrome (Trisomy 21) is the most common chromosomal abnormality among liveborn infants. It is the most frequent form of intellectual disability caused by a microscopically demonstrable chromosomal aberration. Management requires a multidisciplinary approach to the ongoing evaluation and monitoring for associated congenital anomalies and acquired disorders. Trisomy 21 is characterized by a variety of dysmorphic features, congenital anomalies and associated medical conditions. Knowledge of these associated conditions are important for clinicians involved in the management of these patients. Appropriate radiologic imaging with prompt, accurate interpretation plays an important role in the diagnosis and management of these diseases. The primary goal of this pictorial review is to unravel the radiological findings of these associated conditions.

INTRODUCTION

Down syndrome (trisomy 21) is the most commonly recognized genetic cause of intellectual disability, with an incidence of approximately 9.2 cases per 10,000 live births in the United States¹. The risk of trisomy 21 is directly related to maternal age. Molecular genetic studies reveal that 95 percent of occurrences of trisomy 21 result from nondisjunction during meiotic division of the primary oocyte while the remaining cases are due to either translocation or mosaicism (Figure 1). The maternal serum markers used to screen for trisomy 21 are alpha-fetoprotein, unconjugated estriol and human chorionic gonadotropin. At age 35, the second-trimester prevalence of trisomy 21 (1/270) approaches the estimated risk of fetal loss due to amniocentesis (1/200)². Therefore, age 35 was chosen as the screening cutoff. Findings of increased nuchal translucency, choroid plexus cyst, congenital heart defects, increased intestinal echogenicities, increased iliac wing angle, "double bubble sign" seen in duodenal atresia, two vessel umbilical cord, clinodactyly and cystic hygroma on antenatal ultrasound would suggest underlying Trisomy 21¹. A number of congenital malformations and acquired diseases occur with increased frequency in persons with Down syndrome. The primary goal of this pictorial review is to unravel the radiological findings of these conditions which are categorized according to body systems for ease of discussion (Figure 2).

RESPIRATORY AND CARDIOVASCULAR SYSTEMS

Congenital heart disease

Congenital heart disease affects approximately 40% of patients with Trisomy 21, particularly involving the endocardial cushion, of which atrioventricular septal defect (AVSD) is the most common. The essential morphological hallmark of an AVSD is the presence of a common atrioventricular junction as compared to the separate right and left atrioventricular junction in the normal heart. Other morphological features include defects of the muscular and membranous atrioventricular septum and an ovoid shape of the common atrioventricular junction. There is disproportion of outlet and inlet dimensions of the left ventricle, with the former greater than the latter as compared to the normal heart where both dimensions are similar².

Large shunts present early with tachypnea, tachycardia and failure to thrive while small shunts may be well tolerated and may be asymptomatic till late childhood or early adulthood. Clinically, the less severe forms resemble atrial septal defect, but the symptoms in atrioventricular septal defect are frequently more severe.

Chest radiograph would show cardiomegaly with enlarged main pulmonary artery and increased pulmonary arterial blood flow secondary to left-to-right shunting (Figure 3). Echocardiography will demonstrate the size of defect and relative size of the ventricles. Magnetic resonance imaging is a valuable tool for the evaluation of atrioventricular septal defects, among which there is considerable morphologic variation, and is particularly useful in delineating anatomic features important to surgical planning. For example, MR imaging is superior to echocardiography and angiography in depicting the presence and size of the ventricular component of the defect, information that may aid in the timing of surgery³. Cardiac CT is another non-invasive alternative to depict anatomy, chamber volumes and function. Three-dimensional CT reconstructions are useful for depicting complex global anatomy for pre-surgical planning. Cardiac catheterization is not usually performed to evaluate anatomy but to measure pulmonary vascular resistance.

Diaphragmatic hernia

Congenital diaphragmatic hernia (CDH) occurs when the diaphragm fails to close completely during in-utero development, resulting in herniation of abdominal contents into the thoracic cage, preventing normal development of the

This article was accepted: 28 November 2013

*Corresponding Author: Ai Peng Tan, Registrar, National University Hospital, Diagnostic Radiology, 5 Lower Kent Ridge Road, Singapore 119074, Singapore
Email: tan_ai_peng@hotmail.com*

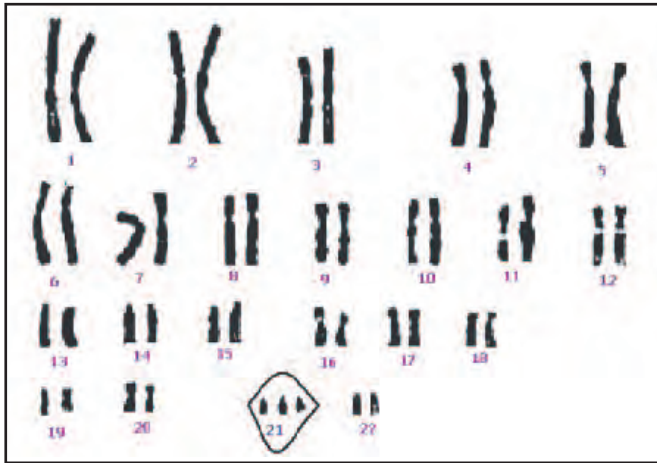


Fig. 1 : Karyotype for Down syndrome where there are 3 instead of the normal 2 copies of chromosome 21, hence the name Trisomy 21. 95% of cases occur as a result of nondisjunction during meiotic division of the primary oocyte.

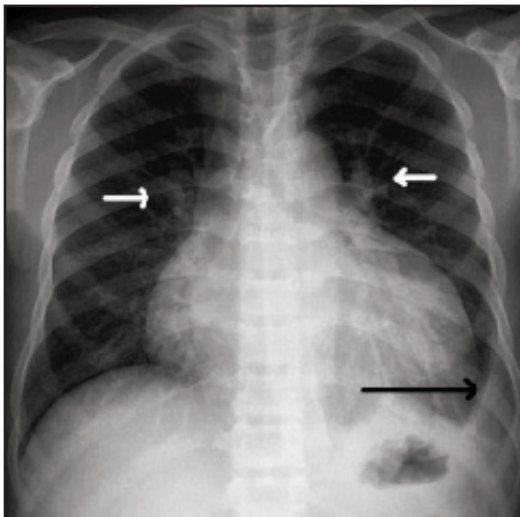


Fig. 3 : Frontal chest radiograph of a 15-year-old male demonstrates cardiomegaly, increased pulmonary vascularity (short white arrows) and a small left pleural effusion (long black arrow). The left main bronchus is elevated due to enlargement of the left atrium. The patient had an untreated small atrioventricular septal defect which results in congestive cardiac failure.

lung. There are two types of congenital diaphragmatic hernia, Morgagni and Bochdalek hernias, the latter being the more common subtype, with an estimated frequency of 1 per 2000–5000 live births⁴.

A Bochdalek hernia is a congenital hernia through a posterolateral defect in the diaphragm. The defect is thought to arise from malformation of the pleuroperitoneal fold or failure of the pleuroperitoneal fold and septum transversum to fuse properly with intercostal muscle. Most Bochdalek hernias (80%) occur on the left side⁵. The primary management consists of mechanical ventilation, with care taken to minimize toxic effects of oxygen and barotrauma. Medical treatment of pulmonary hypertension with nitric

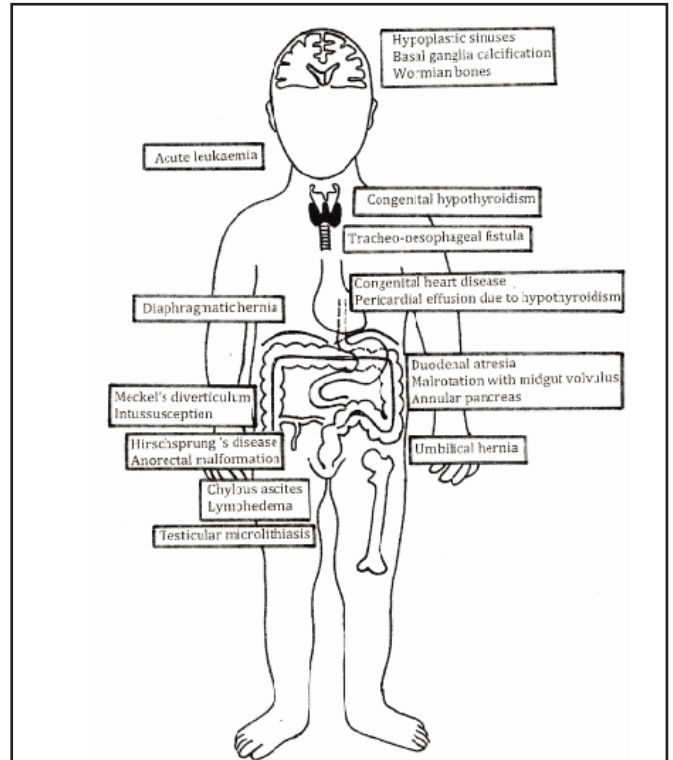


Fig. 2 : Diagrammatic representation of congenital malformations and acquired diseases occur with increased frequency in persons with Down syndrome.

oxide and pharmacologic support of cardiac function are equally important. Once the child's condition has been adequately stabilized, surgical repair is performed.

The foramen of Morgagni is an anterior opening in the diaphragm that extends between the sternum medially and the eighth rib laterally. It is caused by failure of fusion between the transverse septum and the lateral body wall where the internal mammary artery crosses the diaphragm. Hernias through the foramen of Morgagni are mostly unilateral, are right sided in 90% of cases, and account for 9%–12% of diaphragmatic defects in infancy⁴. Most Morgagni hernias are detected in older children and adults as incidental findings or manifest as pulmonary infection or GI obstruction⁴. Surgical repair is performed irrespective of symptoms because of the risk of bowel incarceration and strangulation.

On chest radiograph, one would expect to see herniation of abdominal contents, most commonly bowel loops, into the thoracic cage (Figure 4). Occasionally, there may also be opacification of the affected hemithorax due to herniation of upper abdominal solid organs such as the liver and spleen. On prenatal ultrasound, mass of mixed echogenicities within the thoracic cavity is suggestive of CDH. There is also often displacement of the mediastinum and abnormal position of the stomach. US is however less often utilized in evaluation of CDH in the post-natal period. In cases where other cystic pulmonary masses such as congenital lobar emphysema, congenital pulmonary airway malformation or pulmonary sequestration are suspected, computed tomography (CT)

study may be performed to confirm diagnosis. Fetal magnetic resonance imaging (MRI) enable measurement of fetal lung volume and lung-to-head ratio which are essential for prognostication. Fluoroscopy on the other hand could be utilised to discern between CDH and diaphragmatic eventration.

The overall prognosis for infants with congenital diaphragmatic hernia depends on the severity of pulmonary hypoplasia as well as the presence of other associated congenital anomalies. Liver herniation in left CDH indicates a large defect with early herniation of viscera resulting in severe pulmonary hypoplasia. Liver herniation is one of the most important prognostic factors and indicates poor outcome and greater likelihood of need for extracorporeal membrane oxygenation (ECMO).

GASTROINTESTINAL SYSTEM

Duodenal atresia/stenosis

Duodenal atresia/stenosis is the most common cause of upper gastrointestinal obstruction in neonates and is associated with many congenital syndromes, the foremost being Down syndrome. Approximately 30% of children with duodenal atresia have trisomy 21⁶. There is also an association with anomalies of the VACTERL (vertebral, anorectal, cardiac, tracheoesophageal, renal, and limb anomalies) spectrum. The prevalence of duodenal atresia is one in 10,000 newborns. Although more distal small-bowel atresia is believed to be secondary to an ischemic episode, duodenal atresia is thought to represent a failure of recanalization of the bowel lumen that is a solid tube early in fetal life.

Infants with duodenal atresia present with bilious vomiting early in the neonatal period. The atretic segment is most often just beyond the ampulla of Vater at the junction of foregut and midgut. If the atresia is proximal to the ampulla, the vomiting is nonbilious. If left untreated, it will result in severe dehydration and electrolyte imbalance.

Plain radiograph will demonstrate distention of the stomach and proximal duodenum, giving rise to the classical “double bubble” sign⁷ (Figure 5). Duodenal atresia produces complete obstruction, and, unless an alternative route exists for proximal air to reach the remainder of the small bowel, there is no distal bowel gas. Hence, if a “double bubble” sign is noted with absence of distal gas, a diagnosis of duodenal atresia can be made. On the contrary, if distal gas is present, partially obstructing anomalies such as annular pancreas and malrotation⁸ needs to be excluded before a diagnosis of duodenal stenosis can be confidently made. An upper GI contrast study can be performed to exclude the presence of malrotation. Alternatively, ultrasound can be done to look for sonographic features of malrotation and at the same time exclude the presence of annular pancreas. Further, the biliary tree can be assessed to look for associated biliary anomalies such as choledochal cyst.

Duodenoduodenostomy is the most common surgical treatment with a success rate of approximately 90%. Surgical repair is urgent but not emergent and may be delayed to first address severe cardiac or respiratory insufficiency or to correct electrolyte and fluid balance disturbances.

Malrotation with midgut volvulus

Rotational anomaly of the gut is the result of arrest of gut rotation and fixation during fetal development. In classic malrotation, the caecum lies in the midline or to the left. It is fixed in position by fibrous bands from the undersurface of the liver (Ladd bands). Ladd bands cross the duodenum and may obstruct it. In such instance, plain radiograph will show the “double bubble” sign and may simulate duodenal stenosis.

The diagnosis of malrotation can be made on upper GI contrast study when the duodenojejunal (DJ) junction is seen to the right of the spine. The normal DJ junction should be seen to the left of the spine, superior or at the same level as the duodenal bulb (Figure 6). On the lateral view, the duodenum typically courses posteriorly then inferiorly in normal individuals. When a volvulus is present, the small bowel has a “corkscrew” appearance because it twists around the superior mesenteric artery (figure 7). US, CT, and MR imaging may allow detection of malrotation by showing the superior mesenteric artery and superior mesenteric vein in abnormal relative positions. A superior mesenteric vein that is inverted relative to the superior mesenteric artery is highly indicative of malrotation. Pracros *et al* described the “whirlpool” sign of actual midgut volvulus at color Doppler US, a sign that is characterized by clockwise wrapping of the superior mesenteric vein and mesentery around the superior mesenteric artery (Figure 8)⁹. However, the absence of an abnormal relationship between the superior mesenteric artery and superior mesenteric vein does not totally exclude the possibility of malrotation; moreover, some patients with abnormal relative positions of these vessels do not have malrotation. Thus, an upper gastrointestinal series remains the standard of reference in the diagnosis of malrotation. Midgut volvulus is a surgical emergency as delay in treatment may result in bowel ischemia or infarct.

Hirschsprung disease

Hirschsprung disease (HD) is a form of low intestinal obstruction caused by the absence of normal myenteric ganglion cells in a segment of the colon¹⁰. This condition accounts for approximately 15%–20% of cases of neonatal bowel obstruction¹⁰. About 2% of patients with Hirschsprung disease also have Down syndrome¹⁰. The aganglionosis varies in length but always extends proximally from the anal canal, and the rectosigmoid area is involved in 80% of cases.

In children with HD, the absence of ganglion cells results in the failure of the distal intestine to relax normally. Peristaltic waves do not pass through the aganglionic segment and there is no normal defecation, leading to functional obstruction. Abdominal distention, failure to pass meconium, enterocolitis and bilious vomiting are the predominant signs and symptoms and appear within a few days after birth.

Radiography performed in children with HD yields findings similar to those in other forms of low small bowel obstruction; variable gaseous distention of the colon and small bowel, often with air-fluid levels. Contrast enema is particularly useful in the investigation of distal bowel obstruction in neonates. A transition zone between the narrowed and dilated portions of the colon in the shape of an inverted cone on barium enema study¹⁰ is the most characteristic radiologic

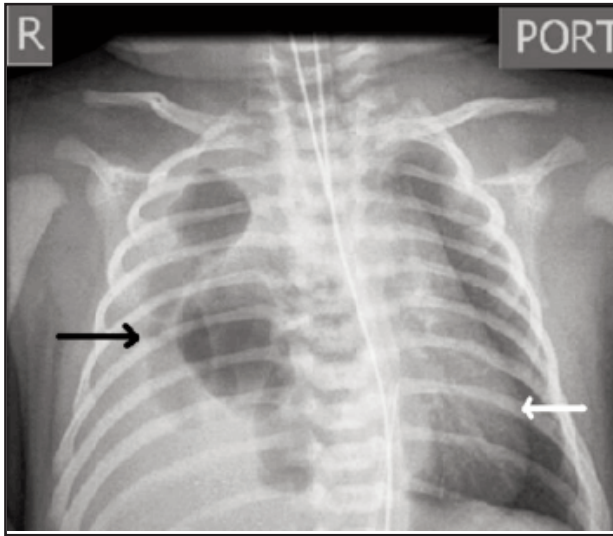


Fig. 4 : Newborn chest radiograph shows herniation of bowel loops into the right thoracic cage (black arrow). The mediastinum is shifted to the left (white arrow) and a right-sided pleural effusion is present.

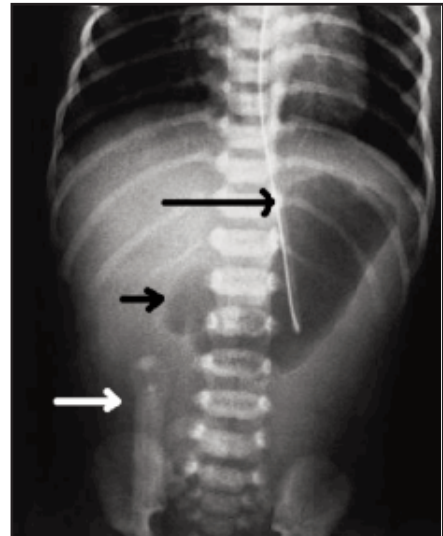


Fig. 5 : Anteroposterior radiograph of the abdomen of a neonate shows marked dilation of the duodenum (short black arrow), which has a rounded configuration when viewed en face. The stomach is also moderately dilated (long black arrow), giving rise to the classical "double bubble" appearance of duodenal stenosis. There is absence of gas beyond the dilated duodenum. An umbilical clamp is noted (white arrow).

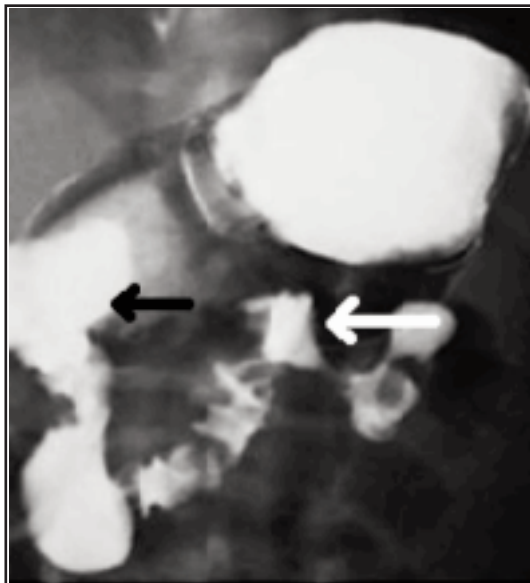


Fig. 6 : Anteroposterior projection of an upper GI study demonstrates the normal duodenojejunal (DJ) junction (white arrow) which is located to the left of the spine and at the same level as the duodenal bulb (black arrow).

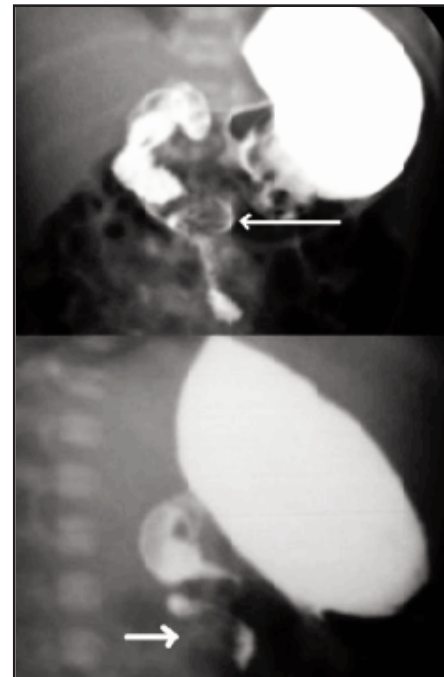


Fig. 7 : Selected anteroposterior and oblique images from an upper GI study show mild dilatation of the proximal duodenum and corkscrew appearance (short white arrow) of the more distal small bowel loop, typical of midgut volvulus. The duodenojejunal junction in this patient with malrotation is sited below the level of the duodenal bulb (long white arrow).

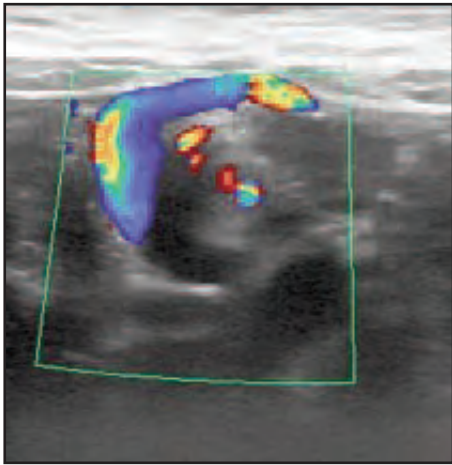


Fig. 8 : Transverse US image demonstrates wrapping of the superior mesenteric vein around the superior mesenteric artery, giving rise to the "whirlpool sign" in a patient with malrotation.

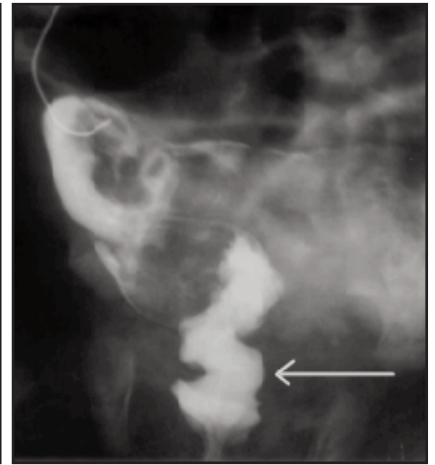
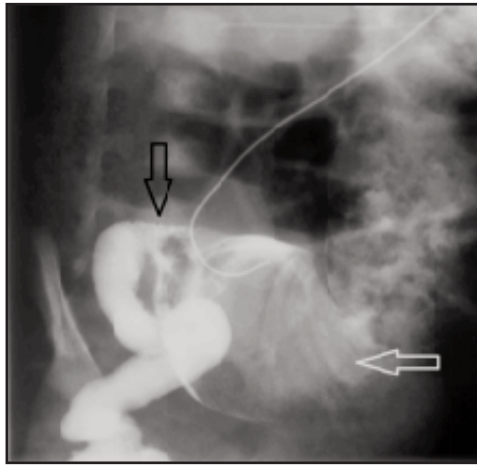


Fig. 9a & b : Serial images from a contrast enema study show the presence of a transition point (black open arrow) between the narrowed and dilated portions (white open arrow) of the colon, at the mid sigmoid colon. Mild fasciculations from spasm is seen within the rectum (white arrow). A short segment Hirschprung's disease was confirmed at rectal biopsy.

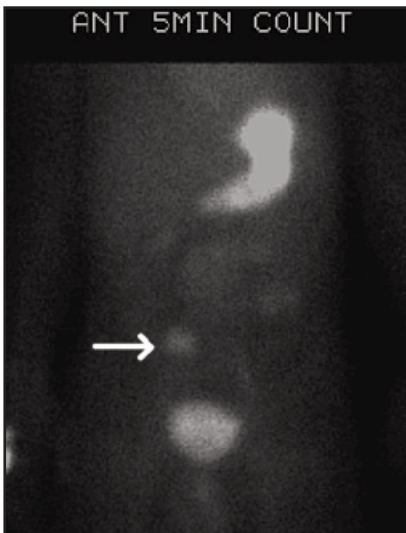


Fig. 10 : Anterior Meckel scan shows a focus of increased radioactivity in the right lower quadrant (white arrow) with intensity that parallels that of the stomach and persists on multiple images (not shown). Findings are in keeping with ectopic gastric mucosa, most likely within a Meckel diverticulum.

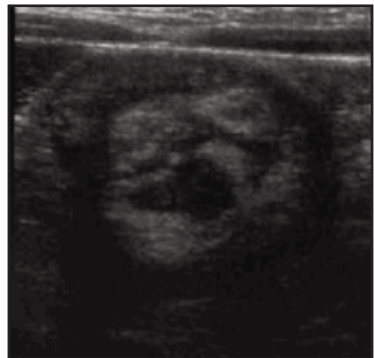
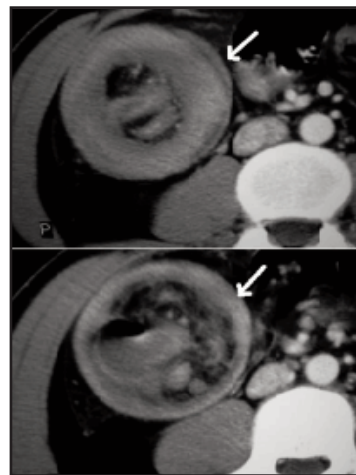
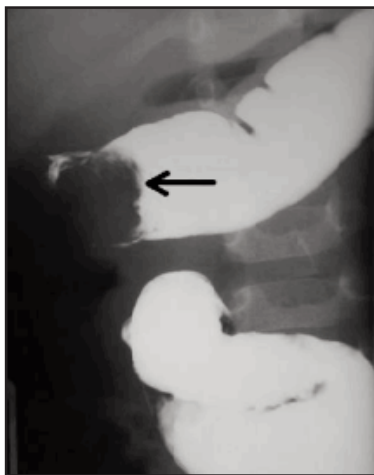


Fig. 11a, b, c : Image from a barium enema (a) study shows the meniscus sign (black arrow), where the rounded apex of the intussusceptum is seen protruding into in the contrast material-filled distal colon. US study of the same patient demonstrates a round mass with alternating concentric rings of hyper- and hypoechoogenicity representing bowel wall and mesenteric fat (b). Contrast enhanced CT study (c) of another patient with ileocolic intussusception shows a soft tissue mass with alternating rings of high and low attenuation in the right upper quadrant (white arrows), consistent with ileocolic intussusception.

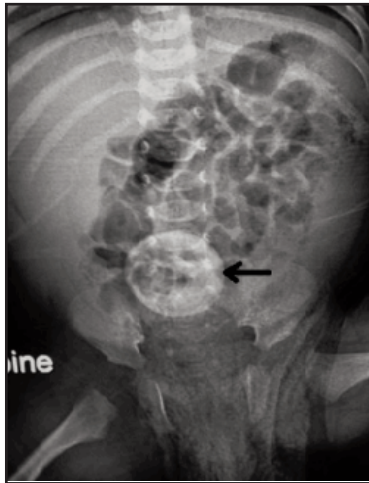


Fig. 12 : Plain radiograph of the abdomen obtained with the patient in a supine position shows a small umbilical hernia (black arrow). This patient was treated conservatively as most congenital umbilical hernia closes spontaneously within 4-6 years of age.

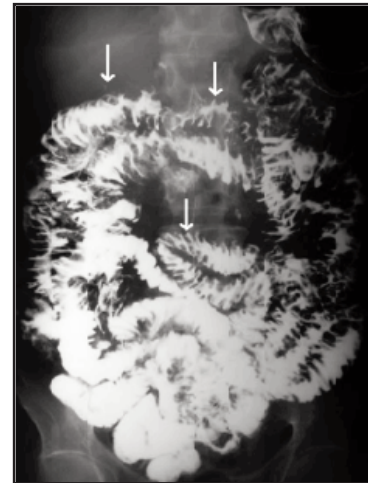


Fig. 13 : Small bowel follow through in a patient with Trisomy 21, done for investigation of unexplained weight loss. Diffuse small bowel fold thickening (white arrows) is noted. Computed tomography (CT) abdomen and pelvis of the same patient (not shown) confirms the presence of small bowel wall thickening, ascites and abdominal wall oedema.

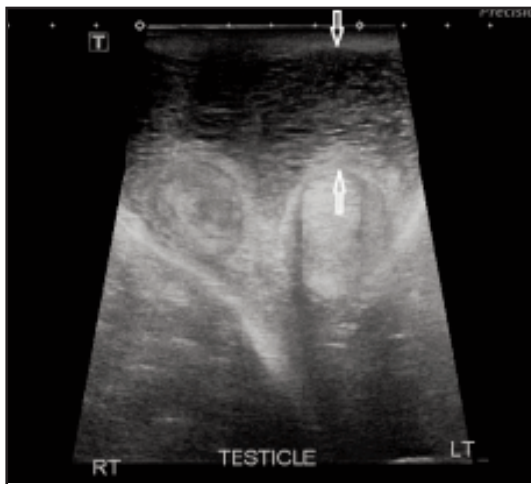


Fig. 14 : Transverse ultrasonography of both scrotal sacs revealed the presence of excess dermal subcutaneous fluid accumulation, seen as layers of alternating hypoechoogenicity and hyperechoogenicity in a patient with Trisomy 21. Patient presented with painless swelling of both scrotal sacs as well as bilateral lower limb oedema.



Fig. 15 : Testicular microlithiasis, arbitrarily defined as five or more microliths on at least one US image, in a patient with Trisomy 21. Ultrasonography depicts multiple tiny punctate echogenic foci throughout the right testis (red arrow). At histologic examination, these represent laminated calcium deposits in the lumina of seminiferous tubules.

finding in HD (Figure 9a). However, the distention of the bowel proximal to the segment of deficient innervation is gradual, and a transition zone is seen in only 50% of neonates during the first week of life. Other findings described on barium enema study include a rectosigmoid ratio of less than 1, sawtooth appearance of denervated colon due to muscle spasm (Figure 9b), irregular or thickened wall with associated colitis and delayed (> 24-48 hours) evacuation of contrast material. Rectal biopsy is needed for definitive diagnosis. Untreated HD may lead to chronic constipation, enterocolitis, toxic megacolon, sepsis or death. Hence, accurate diagnosis is of utmost importance to enable timely surgical management.

Meckel diverticulum

Meckel diverticulum is the remnant of an improperly closed omphalomesenteric duct, arising from the antimesenteric side of the terminal ileum within 2 feet of the ileocaecal valve. It is the most common congenital gastrointestinal tract anomaly, affecting approximately 2-3% of the population¹¹, with increased incidence in patients with Trisomy 21. Meckel diverticulum is a true diverticulum, composed of all layers of the intestinal wall, and is lined by normal small intestinal mucosa¹¹. The presence of ectopic gastric mucosa within the diverticulum may result in painless gastrointestinal bleeding, the most common presenting symptoms in the pediatric population. Clinical symptoms may also arise from

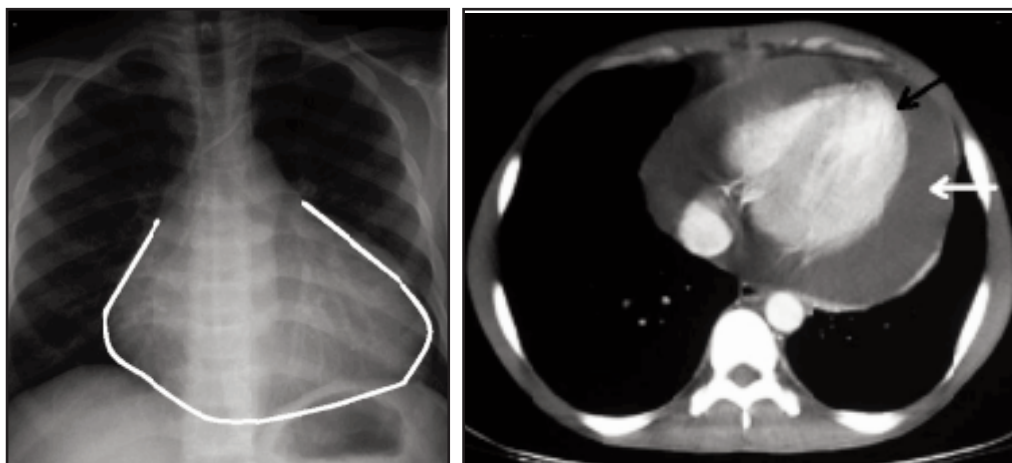


Fig. 16a, b : Posteroanterior chest radiograph (a) demonstrates a globular shaped cardiac silhouette (outlined in white). Contrast enhanced CT scan (b) of the thorax confirms the presence of fluid within the pericardial space (white arrow), in keeping with pericardial effusion. Pericardial fluid is seen compressing upon the cardiac chambers (black arrow).

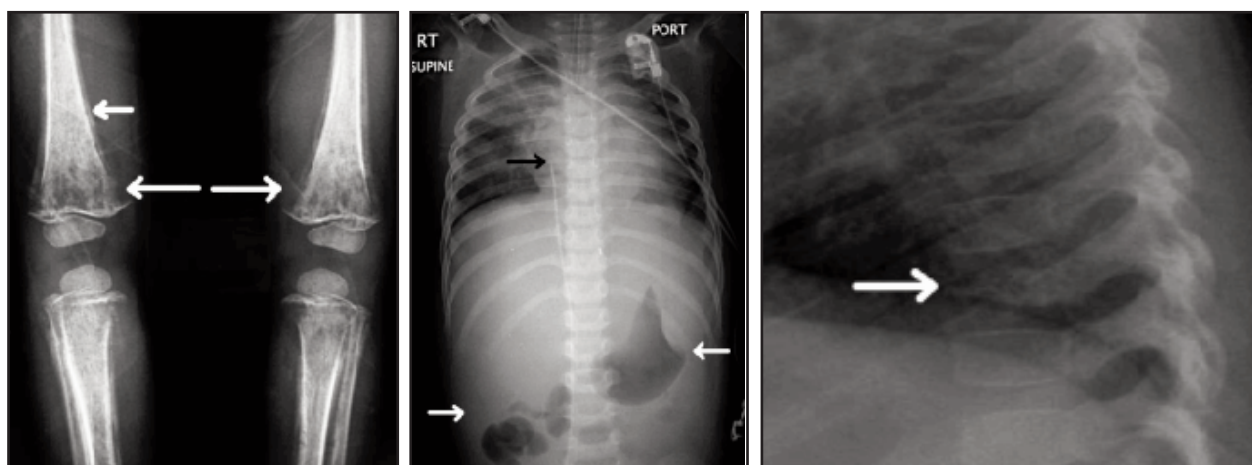


Fig. 17a, b, c :Anteroposterior radiograph of both knees (a) shows ill-defined metaphyseal lucency (long white arrows) and single lamina periosteal reaction (short white arrow) in this child with acute lymphocytic leukemia (ALL). Chest radiograph of the same patient (b) shows hepatosplenomegaly (white arrow) with inferior displacement of the gastric bubble. The tip of the venous catheter is seen within the right atrium (black arrow). Of note is also the presence of vertebra plana in the lower thoracic spine (c).

complications of the diverticulum such as diverticulitis; intestinal obstruction from diverticular inversion, intussusception, volvulus, torsion, or inclusion of the diverticulum in a hernia; formation of enteroliths; and development of neoplasia within the diverticulum¹¹.

Meckel scan (Technitium-99m pertechnetate scan) is the most specific test for Meckel diverticulum with an accuracy of up to 90%. It enable us to detect the presence of ectopic gastric mucosa but not the diverticulum itself. Classic imaging appearance is focal increased activity in the right lower quadrant, which appear with a time course matching that of the stomach due to the presence of ectopic gastric mucosa (Figure 10). An intestinal duplication cyst containing gastric mucosa may yield similar findings. However, this will not have much clinical implication as the treatment of both

conditions will be the same, both of which would be surgically resected.

Intussusception

Intussusception is one of the most common causes of acute abdomen in infancy. Intussusception occurs when a segment of proximal bowel (intussusceptum) invaginates into the lumen of distal bowel (intussusciens) in a telescope-like manner. This condition usually occurs in children between 6 months and 2 years of age¹². In this age group, intussusception is idiopathic in 90% of case, likely secondary to lymphoid hyperplasia. 5-10% of intussusception are caused by pathologic lead points such as Meckel diverticulum, duplication cyst, polyp and lymphoma. The vast majority of childhood cases of intussusception are ileocolic intussusception.

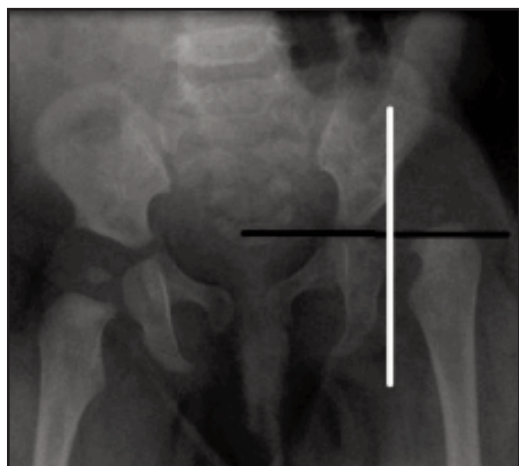


Fig. 18 : Radiograph of the pelvis of a skeletally immature patient shows superolateral displacement of the left femoral head. The left femoral head is projected in the upper outer quadrant formed by the Hilgenreiner line (black line) and Perkin line (white line). The Hilgenreiner line is a horizontal line across the triradiate cartilage while the Perkin line is a line perpendicular to it, drawn at the outer acetabular margin. The degree of ossification of the femoral epiphysis on the left side is decreased compared to the right.

The classic clinical triad of acute abdominal pain, currant-jelly stools or hematochezia, and a palpable abdominal mass is present in less than 50% of children with intussusception. The onset of nonspecific abdominal symptoms in which vomiting predominates, the absence of passage of blood via the rectum (usually in cases of less than 48 hours duration), and the inability to obtain a reliable history from these nonverbal children lead to dismissal of the diagnosis of intussusception in almost 50% of cases¹².

The most common radiographic sign of intussusception is a soft-tissue mass, which is most often seen in the right upper quadrant. The most specific plain radiographic findings are the target sign and meniscus sign. The target sign consists of a soft-tissue mass that contains concentric circular or nearly circular areas of lucency, which are due to the mesenteric fat of the intussusceptum. The meniscus sign on the other hand consists of a crescent of gas within the colonic lumen that outlines the apex of the intussusception (the intussusceptum). Conversely, identification of a cecum filled with gas or feces in the normal location is the finding that allows exclusion of intussusception with the most confidence. The classic signs of intussusception at barium enema examination are the meniscus sign and coiled spring sign. The meniscus sign at enema examination is analogous to the meniscus sign at plain radiography and is produced by the rounded apex of the intussusceptum protruding into the column of contrast material (Figure 11a). The coiled spring sign is produced when the edematous mucosal folds of the returning limb of the intussusceptum are outlined by contrast material in the lumen of the colon.

Grayscale ultrasonography has a 97-100% accuracy in diagnosis of intussusception. On transverse sonography, intussusception is seen as a round mass with alternating

concentric rings of hyper- and hypoechogenicity representing bowel wall and mesenteric fat (Figure 11b). On longitudinal sonography, ovoid mass with alternating layers of hyper- and hypoechogenicity gives rise to the pseudokidney sign. Trapped fluid within intussusception is associated with higher enema reduction failure rate and increased likelihood of bowel necrosis.

On computed tomography (CT), intussusception is seen as a soft tissue mass with alternating rings of high and low attenuation, most commonly in the right upper quadrant (Figure 11c).

Umbilical hernia

Umbilical hernia is defined as midline protrusion of abdominal contents into or through the anterior abdominal wall via the umbilical ring. Umbilical hernias usually occur in the upper half of umbilicus and are usually small in size¹³. The most common presenting complaint would be that of a mass protruding through the umbilicus, typically enlarges on coughing or straining. 80% of the congenital subtype closes spontaneously within 4-6 years of age¹³. The possible complications of abdominal wall hernias include bowel obstruction, incarceration and strangulation. These are however very rare in congenital umbilical hernia. Physical examination may reveal a firm, tender abdominal wall mass. Abdominal distention, dehydration or peritonitis manifest later in the course of the disease.

Multi-detector computed tomography (CT) with its multiplanar capabilities is particularly useful for the evaluation of abdominal wall hernias and for treatment planning. Multi-detector CT provides exquisite anatomic detail of the abdominal wall, thereby allowing accurate identification of wall hernias and their contents, differentiation of hernias from other abdominal masses (tumors, hematomas, abscesses) and detection of complications such as bowel ischemia and obstruction¹³. Findings of bowel ischemia such as bowel wall thickening, abnormal mural enhancement, vessel engorgement, mesenteric haziness and ascites are readily identified on CT imaging.

Among the few indications for surgical repair of congenital umbilical hernia are hernia which persists beyond 5 years of age, hernia incarceration and a defect larger than 2 cm.

LYMPHATIC SYSTEM

Lymphedema

Lymphedema may occur in patients with Trisomy 21 due to underlying lymphatic dysplasia. In the past, corroboration of the nature and extent of lymphatic dysfunction required the cumbersome and inconvenient procedure of conventional lymphography¹⁴. Despite this background of frustration in lymphedema diagnosis and treatment, the availability of newer imaging techniques and the increasing number of treatment options now dictate that the prevailing approach be revisited.

Most patients with lymphedema have either unilateral or bilateral limb swelling (involving the legs more often than the arms)¹⁴. In some patients with lower-extremity

lymphedema, lymphatic dysplasia also involves the viscera, and peripheral edema is compounded by reflux of retroperitoneal and even mesenteric (intestinal) lymph. Lymphangiographic findings in affected patients vary considerably¹⁴.

In intestinal lymphedema, barium small bowel follow through would reveal diffuse small bowel fold thickening (Figure 13). Unfortunately, this barium examination pattern is not specific, and barium studies of the small bowel are no longer commonly performed. The number of barium examinations performed and the skill necessary to interpret their results are both in decline. On computed tomography (CT), one would expect to see diffuse small bowel wall thickening with submucosal edema, giving rise to the "halo" sign of edema between enhanced mucosa and serosa. Not uncommon are other associated findings such as infiltration of the small bowel mesentery, ascites and subcutaneous oedema of the abdominal wall.

Patients with scrotal lymphedema present with painless scrotal swelling, unless superimposed infection is present. The scrotal wall is composed of the following structures, listed from the superficial to the deep layers: rugated skin, superficial fascia, dartos muscle, external spermatic fascia, cremasteric fascia, and internal spermatic fascia. The normal scrotal wall thickness is approximately 2–8 mm, depending on the state of contraction of the cremasteric muscle. In scrotal lymphedema, the scrotal wall appears thickened, with layers of alternating hypoechogenicity and hyperechogenicity (Figure 14).

GENITOURINARY SYSTEM

Testicular microlithiasis

Testicular microlithiasis is a relatively rare entity, reported to be present on approximately 0.6% of testicular sonograms¹⁵. Testicular microlithiasis has been associated with Klinefelter syndrome, male pseudohermaphroditism, Down syndrome (Trisomy 21), subfertility, infertility, cryptorchism, hypogonadism, and pulmonary microlithiasis.

At ultrasonography (US), microliths appear as tiny punctate echogenic foci which typically do not cause posterior acoustic shadowing. Testicular microlithiasis is defined as five or more microliths on at least one US image¹⁵ (Figure 15). Histologically, these represent scattered laminated calcium deposits in the lumina of the seminiferous tubules. Multiple investigators have reported an association between testicular microlithiasis and testicular cancer. Given this association, most centers currently recommend that patients with testicular microlithiasis undergo regular follow-up with physical examination and US at least annually.

Testicular microlithiasis has been described as two histologic types of intratesticular microcalcifications. One type of microcalcification is the hematoxylin body consisting of amorphous calcific debris, which is associated with germ cell tumors and thought to be the result of a rapid cell turnover. The other type of microcalcification is laminated calcifications, which are found in association with germ cell tumors, cryptorchid testes, and otherwise normal testes.

ENDOCRINE

Hypothyroidism

Clinical forms of hypothyroidism found in individuals with Down syndrome include transient and primary hypothyroidism, pituitary-hypothalamic hypothyroidism, thyroxin-binding globulin (TBG) deficiency and chronic lymphocytic thyroiditis¹⁶. Hyperthyroidism also occurs occasionally. The frequency of thyroid disease is elevated in patients with Down syndrome, starting in the newborn population where it is 0.7% or 28 times more frequent than in the general population¹⁶. Twelve per cent or more of adults with Down syndrome have thyroid disease¹⁶. Thyroid disease is difficult to diagnose clinically in individuals with Down syndrome because of an overlap of symptoms. This makes thyroid blood screening a particularly important part of the annual preventive medicine screening of person with Down syndrome.

Pericardial effusion is reported to occur in 30% to 80% of subjects with hypothyroidism¹⁷. Pericardial effusion may be a frequent manifestation in myxedema, an advanced stage of hypothyroidism but is rarely seen in early stage of hypothyroidism (Figure 16). The thickness of the normal pericardium, measured on CT scans and on MR images, is less than 2 mm. Echocardiography is considered the primary imaging modality for the evaluation of pericardial effusion because of its high sensitivity and specificity, lack of ionizing radiation, easy accessibility and low cost. CT and MR imaging are indicated when loculated or hemorrhagic effusion or pericardial thickening is suspected or when findings at echocardiography are inconclusive. Loculated effusions, especially those in anterior locations, can be difficult to detect at echocardiography but are readily demonstrated at CT or MR imaging, both of which provide a wider field of view. Both CT and MR imaging provide excellent delineation of the pericardial anatomy and can aid in the precise localization and characterization of various pericardial lesions, including effusion, constrictive pericarditis and pericardial thickening.

IMMUNE SYSTEM

Leukaemia

Acute leukaemia is the most common malignancy in children and comprises about 41% of malignancies in children younger than 15 years old. It is the second most common malignancy in children under one-year-old. Acute lymphocytic leukemia (ALL) is responsible for approximately 23% of all cancers and 76% of leukemia in this age group. The peak age of involvement is 2-6 years and boys are slightly more involved than girls. Chromosomal abnormalities such as Trisomy 21, ataxia telangiectasia, Bloom and Fanconi syndromes are prone to this malignancy. Leukemic cells proliferate within the massive red bone marrow in children.

Children with acute lymphoblastic leukemia (ALL) often present with signs and symptoms that reflect bone marrow infiltration and/or extramedullary disease. When leukemic blasts replace the bone marrow, patients present with signs of bone marrow failure, including anemia, thrombocytopenia, and neutropenia. Occasional, patient may also present with pathological fracture and hepatosplenomegaly from extramedullary hematopoiesis (Figure 17b).

Findings on musculoskeletal radiography include metaphyseal lucent band and erosion, periosteal reaction, lytic lesion with permeative margins, generalised reduced bone density and collapsed vertebra (vertebra plana)(Figure 17a,c).

Recent therapeutic advances such as aggressive polychemotherapy, intrathecal cytostatic prophylaxis, and cranial irradiation have improved the prognosis of acute leukemia. Bone marrow transplantation, with the possibility of eradicating remaining malignant cells and suppressing the recipient's immune system, has also revolutionized the treatment of these patients.

MUSCULOSKELETAL SYSTEM

Congenital hip dislocation

Congenital dysplasia of the hip (CDH) also known as developmental dysplasia of the hip (DDH) refers to an abnormal configuration of, or relationship between, the femoral head and the acetabulum¹⁸. It is a continuum of disorders that ranges from shallowness of the acetabulum, to instability and subluxation of the femoral head, to frank dislocation. In 2% of cases the hip dislocation is not evident at birth but manifest in first few months of the life. Hip instability is more common in certain congenital or genetic conditions associated with ligamentous laxity such as Down syndrome

Clinical examination, plain radiography and ultrasonography are useful for the diagnosis of DDH in neonates. A positive ortolani test is a palpable shift as the dislocated femoral head is reduced into the acetabulum with abduction of hip. The Barlow test is performed with the hip in an adducted position. With gentle posterior pressure, a palpable shift should be felt as the hip subluxes out of the acetabulum. A positive Ortoloni or Barlow test indicates DDH.

The anteroposterior (AP) pelvic radiograph is useful after the formation of secondary ossification center of the proximal femur. A horizontal line (Hilgenreiner's line) is drawn between the triradiate cartilages. A vertical line (Perkin's line) perpendicular to the Hilgenreiner's line through the superolateral edge of the acetabulum divides the hip into 4 quadrants. The proximal medial femur or the ossification center of the femoral head, if present (usually observed in patients aged 4-7 months), should be in the lower medial quadrant. The acetabular angle is an angle between the Hilgenreiner line and a line drawn from the triradiate epiphysis to the lateral edge of the acetabulum. Typically this angle decreases with age and should measure less than 20 degrees by the time the child is 2 years old.

Ultrasonography (US) is considered the imaging technique of choice for the diagnosis of DDH in the neonate and infant. The Graf index is widely used in interpretation of US findings, combining both α and β angles. The α angle determines the type while the β angle determines the subtype. Hips with an α angle of 60° or larger are considered normal as are

neonatal hips with an α angle of 50° or larger. Additional variables can be obtained from dynamic manoeuvre, for instance, the degree of femoral head displacement in relation to the acetabulum when transverse force is applied.

The goal of treatment is to obtain a reduction to provide an optimal environment for femoral head and acetabular development.

CONCLUSION

Down syndrome (Trisomy 21) being the most common chromosomal abnormality among liveborn infants, is associated with a number of congenital malformations. In addition, several acquired diseases occur with increased frequency in persons with Down syndrome. Hence, management of these patients requires an organized multidisciplinary approach and continuous monitoring, of which radiologic imaging plays a vital role. The primary goal of this pictorial review is to unravel the radiological findings of these conditions which are categorized according to body systems for ease of discussion and understanding.

REFERENCES

1. Newberger DS. Down Syndrome: Prenatal Risk Assessment and Diagnosis. *Am Fam Physician*. 2000; 62(4): 825-32.
2. Craig B. Atrioventricular septal defect: from fetus to adult. *Heart*. 2006; 92(12): 1879-85.
3. Parsons JM, Baker EJ, Anderson RH, et al. Morphological evaluation of atrioventricular septal defects by magnetic resonance imaging. *Br Heart J*. 1990; 64: 138-45.
4. GB. Chavhan PS, Babyn, RA. Cohen et al. Multimodality Imaging of the Pediatric Diaphragm: Anatomy and Pathologic Conditions. *Radiographics*. 2010; 30: 1797-817.
5. Taylor GA, Atalabi OM, Estroff JA. Imaging of congenital diaphragmatic hernias. *Pediatr Radiol*. 2009; 39(1): 1-16.
6. Rudolph C. Congenital atresias, stenosis and webs. *Rudolph's pediatrics*. 20th ed. Stamford, Conn: Appleton & Lange, 1996; 1069.
7. Traubici J. The Double Bubble Sign. *Radiology*. 2001; 220: 463-4.
8. Leonidas JC, Berdon W. The neonate and young infant: the gastrointestinal tract. *Caffey's pediatric x-ray diagnosis*. 9th ed. St Louis, Mosby :1993; 2048-55.
9. Pracros JP, Sann L, Genin G, et al. Ultrasound diagnosis of midgut volvulus: the "whirlpool" sign. *Pediatr Radiol*. 1992; 22(1): 18-20.
10. T. Berrocal, M. Lamas, J. Gutiérrez et al. Congenital Anomalies of the Small Intestine, Colon, and Rectum. *Radiographics*. 1999; 19: 1219-36.
11. AD. Levy, CM. HobbsMeckel Diverticulum: Radiologic Features with Pathologic Correlation. *Radiographics*. 2004; 24: 565-87.
12. G-Pozo, JC. Albillos, D. Tejedor et al. Intussusception in Children: Current Concepts in Diagnosis and Enema Reduction. *Radiographics*. 1999; 19: 299-319.
13. Aguirre DA, Santosa AC, Casola G, Sirlin CB. Abdominal Wall Hernias: Imaging Features, Complications, and Diagnostic Pitfalls at Multi-Detector Row CT. *Radiographics*. 2005; 25: 1501-20.
14. Witte CL, Witte MH, Unger EC, Williams WH, Bernas MJ, et al. Advances in Imaging of Lymph Flow Disorders. *Radiographics*. 2000; 20: 1697-719.
15. Bennett HF, Middleton WD, Bullock AD, Teeffey SA. Testicular Microlithiasis: US Follow-up. *Radiology*. 2001; 218: 359-63.
16. Coleman M. Thyroid dysfunction in Down syndrome: A review. *Down Syndrome Research and Practice*. 1994; 2(3): 112-5.
17. Kabadi UM, Kumar SP. Pericardial effusion in primary hypothyroidism. *Am Heart J*. 1990; 120: 1393-5.
18. J Iqbal. Congenital dislocation of the hip. *NMJ*. 2009; 1(4): 16-23.
19. Long FR, Kramer SS, Markowitz RI. Radiographic patterns of intestinal malrotation in children. *Radiographics*. 1996; 16: 547-56.
20. Higgins CB, Byrd BF, Farmer DW, Osaki L, Silverman NH, et al. Magnetic resonance imaging in patients with congenital heart disease. *Circulation*. 1984; 70: 851-60.